

# The Growth and Properties of Pd and Pt on Al<sub>2</sub>O<sub>3</sub>/NiAl(110)

M. Bäumer\*), J. Libuda, A. Sandell, and H.-J. Freund

Lehrstuhl für Physikalische Chemie I, Ruhr-Universität Bochum, Universitätsstraße 150, D-44780 Bochum, Germany

G. Graw, Th. Bertrams<sup>1)</sup>, and H. Neddermeyer<sup>1)</sup>

Experimentalphysik, Ruhr-Universität Bochum, Universitätsstraße 150, D-44780 Bochum, Germany

<sup>1)</sup> Fachbereich Physik, Martin-Luther-Universität, Friedemann-Bach-Straße 6, D-06108 Halle, Germany

**Key Words:** Adsorption / Electron Diffraction / Scanning Tunneling Microscopy / Supported Particles / Surfaces

Small metal particles have strongly size-dependent properties, which – in the case of supported particles – are also influenced by the particle substrate interaction. We have investigated such effects for Pd deposited on a thin alumina film grown on NiAl(110) by probing the adsorption behaviour of CO. Structure and size of the metal islands were varied by employing different substrate temperatures during evaporation. We found that at 90 K small, disordered aggregates are formed, whereas deposition at 300 K results in larger crystallites with (111) facets. The CO thermal desorption spectra show a size-dependent behaviour which can be attributed to a higher degree of CO coordination with decreasing particle size. The results are compared with the corresponding behaviour of Pt. In contrast to Pd, Pt leads to a strong interaction with the substrate at 300 K. This gives rise to a desorption feature of CO in a temperature range which is typical for transition metal oxides.

## 1. Introduction

Adsorption and reaction on small metallic particles often differ strongly from the behaviour of macroscopic metal surfaces. Especially, the interaction of adsorbates with highly dispersed metals on non-metallic supports is of interest, since such systems are of great importance in heterogeneous catalysis [1]. While the adsorption behaviour of large crystals is usually well understood from numerous studies on single crystals [2], very little is known about supported metal clusters and islands.

In order to get some insight into the relationship between the geometric structure of metal deposits and their adsorption properties, we carried out an investigation of Pd on a thin alumina film grown on NiAl(110). The essential properties of this film, which has been extensively characterised in former investigations [3, 4], are listed in Table 1. By using a film instead of a oxide single crystal, we had the unique opportunity to apply electron spectroscopic techniques and electron diffraction since charging could be avoided.

Table 1  
Summary of the essential properties of the alumina film used for metal deposition in this study

Subject	Properties	Ref.
Unit cell	Large, 17.9 Å × 10.6 Å, commensurate along [110], incommensurate along [001]	[3]
Structure	O <sup>2-</sup> anions arranged in a quasi-hexagonal arrangement; distribution of Al <sup>3+</sup> cations similar to γ-Al <sub>2</sub> O <sub>3</sub>	[4]
Defect structure	Two rational domains; antiphase domains	[3]
Thickness	Approximately 5 Å	[3]

The structure and size of the deposits were varied by employing different substrate temperatures during evaporation. The resulting particles were characterised by scanning tunnelling microscopy (STM) and spot profile analysis of LEED reflexes (low-energy electron diffraction). In order to probe the cluster adsorbate interaction, we performed TDS (thermal desorption spectroscopy) with CO as test molecules.

A comparison with preceding studies for Pt on the same substrate [5] demonstrates that the particle substrate interaction being different for both cases can play a significant role for the adsorption behaviour.

## 2. Experimental

We performed the experiments in two different ultrahigh vacuum systems. The LEED investigations were carried out in a chamber equipped with a Leybold SPA-LEED system (specified transfer width: 900 Å, typical primary beam currents: 50 pA – 1 nA). All spot profiles shown in the following have been recorded along the [001]-direction of the NiAl substrate. However, the scaling of the plots refers to the NiAl reciprocal lattice vector along [110], i.e. the distance between the (00) and the (01) spot (1.54 Å<sup>-1</sup>), which has been used for k-space calibration of the SPA-LEED instrument.

Thermal desorption measurements were carried out with a differentially pumped mass spectrometer, which was equipped with a conical aperture (about 5 mm diameter) eliminating molecules not directly desorbing from the sample surface. During the experiment, the crystal was positioned approximately 0.3 mm from the aperture and heated from behind by radiation from a filament. The heating rate was about 1.5 Ks<sup>-1</sup>.

The STM images have been taken with a variable temperature STM designed for the range between approximately 10 K and room temperature. In the present experiments, the

\*) Corresponding author. Fax: +49(234)7094182

cryostat was cooled with liquid nitrogen resulting in a minimum temperature of about 80 K. Furthermore, the system was equipped with a LEED/AES optics.

The clean NiAl(110) surface was prepared by several cycles of sputtering (Ar<sup>+</sup> ions, 500 eV) and annealing. Cleanliness and composition of the surface was checked by AES.

The ordered Al<sub>2</sub>O<sub>3</sub> film was obtained as previously reported in the literature [4]. After dosing 1200 L O<sub>2</sub> at a sample temperature of 550 K, the crystal was annealed to 1200 K. Afterwards, the quality of the oxide was checked via its LEED profiles and intensities (LEED chamber) [3]. A simple tool of controlling that the oxidation of the surface is complete is provided by CO-TDS, since no CO adsorbs on the clean oxide film at 90 K, whereas CO desorption from non-oxidized NiAl is observed at 300 K [4].

Pd metal (Heraeus, >99.95%) was deposited with two different types of evaporators. The evaporator used for the STM measurements was a Knudsen cell with an alumina crucible, while the one used for the LEED investigation was a commercial evaporator (Omicron) based on electron bombardment and allowing evaporation from a rod. The latter was calibrated by a quartz microbalance. The deposition rates varied between 1.2 and 2.4 Å min<sup>-1</sup> (1 Å Pd corresponds to 6.8 10<sup>14</sup> atoms cm<sup>-2</sup>).

### 3. Results

#### 3.1 Deposition of Pd: Growth at Different Substrate Temperatures

In this section, the SPA-LEED and STM results concerning the growth of Pd on the alumina film will be described. Starting with the situation at 300 K and turning then to the situation at 90 K, it will become evident that the structure of the Pd particles is strongly dependent on the substrate temperature during deposition.

As shown in Fig. 1, three major changes can be observed within the LEED pattern upon deposition of Pd at room temperature:

- The spots of the oxide pattern gradually vanish excluding an epitaxial growth of Pd on the oxide substrate (a).
- For large amounts of deposited material, extra spots appear forming two rotated hexagons (b). The lattice constant calculated from these extra spots is consistent with Pd(111).
- In addition to that, the shape of the (00) reflex changes upon deposition (c). Apart from a sharp central spike, a diffuse shoulder develops.

From the first two points, it can be concluded that deposition at 300 K results in a three-dimensional growth mode connected with the formation of Pd(111) crystallites which are azimuthally aligned to the oxide: their orientation coincides with the direction of the close packed rows of the distorted oxygen lattice. For the growth of islands and small particles on a surface, it is known that the LEED spot profiles consist of a central spike and a diffuse shoulder [6].

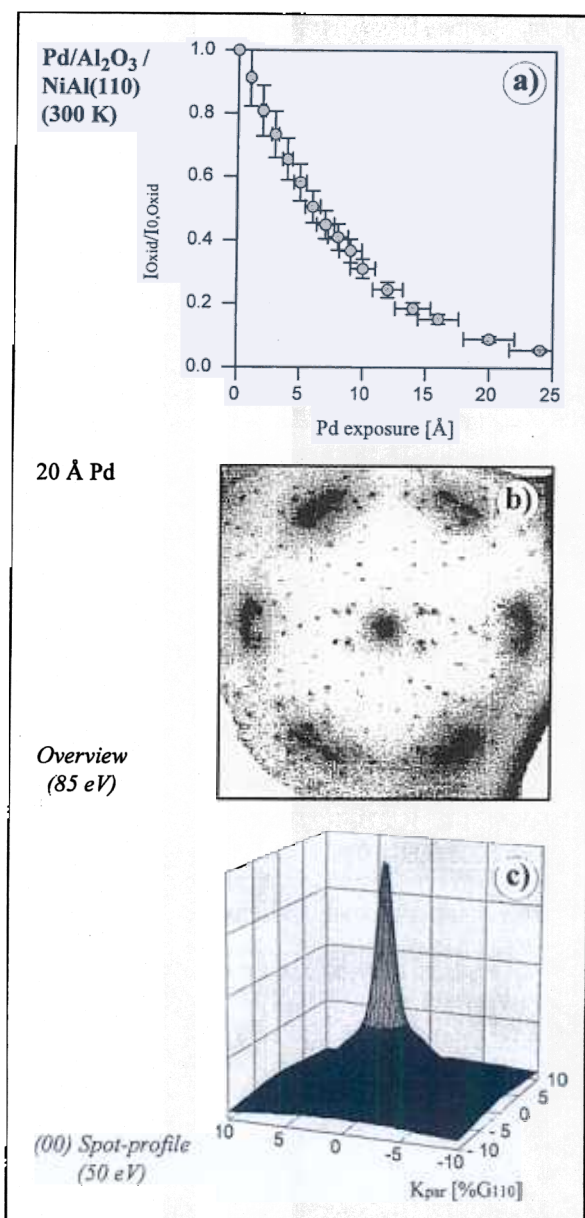


Fig. 1 Changes in the LEED pattern upon deposition of Pd on Al<sub>2</sub>O<sub>3</sub>(111)/NiAl(110) at 300 K: damping of the oxide LEED pattern (a), development of new reflexes forming two rotated hexagons for high Pd exposures (b), development of a diffuse shoulder around the (00) reflex (c)

In Fig. 2a two profiles are compared demonstrating the energy dependence of the profile. At 33 eV – an in-phase energy with respect to the Pd(111) interlayer distance (s. inset) –, the shoulder is narrow, while it is broad at the next out-of-phase energy of 50 eV. This can be understood in terms of monoatomic steps on the Pd islands: in this case, destructive interference between different metal layers gives rise to additional contributions to the shoulder at out-of-phase energies leading to a larger halfwidth. At in-phase energies, on the other hand, steps on the islands do not contribute to the diffuse shoulder. Consequently, these profiles

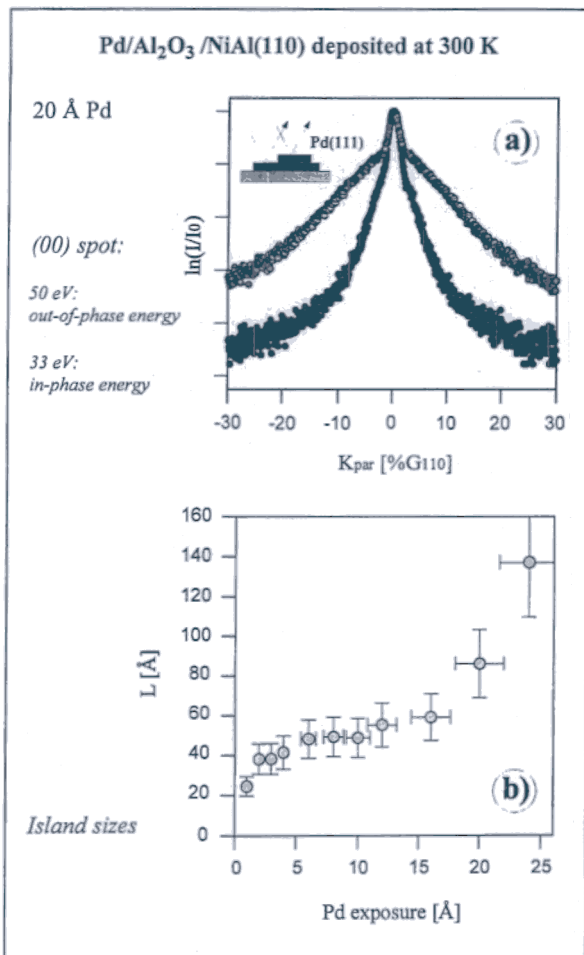


Fig. 2  
Deposition at 300 K: (a) LEED spot profiles of the (00) reflex for an in- and out-of-phase energy with respect to the Pd(111) interlayer distance as illustrated in the inset. (b) Calculated island diameters (see appendix)

can be analysed with a two-layer model: one layer being the oxide substrate and one the Pd-covered areas. Within such a model, the island sizes were estimated as described in the appendix.

The results are graphically displayed in Fig. 2b: after a regime at low exposures, where the growth is determined by nucleation processes, the size of the crystallites is increasing very slowly (compatible with a three-dimensional growth) ranging from 40 to 50 Å. For high exposures, however, coalescence leads to a rapid rise again.

The STM image shown in Fig. 3 corroborates the LEED analysis but also provides complementary information. Obviously, the particles grow according to a Vollmer-Weber growth mode: the crystallites visible are about 50 Å as calculated from the spot profile analysis for a wide range of Pd exposures. Their shape is triangular in many cases: this is consistent with crystallites exposing (111) facets. Moreover, additional pictures at lower coverages reveal that Pd preferentially nucleates at defects like steps and domain boundaries.

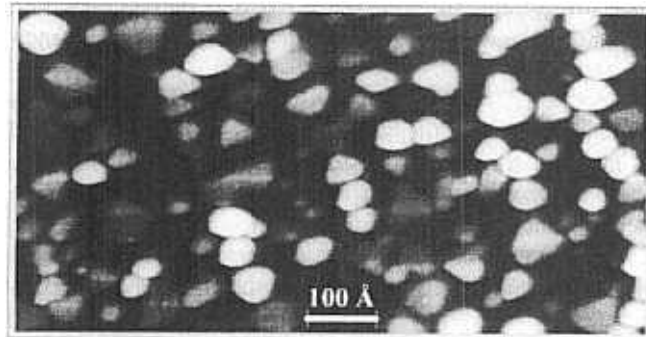


Fig. 3  
STM image (CCT,  $U = 0.4$  V,  $I = 0.5$  nA) of the Pd crystallites deposited at 300 K

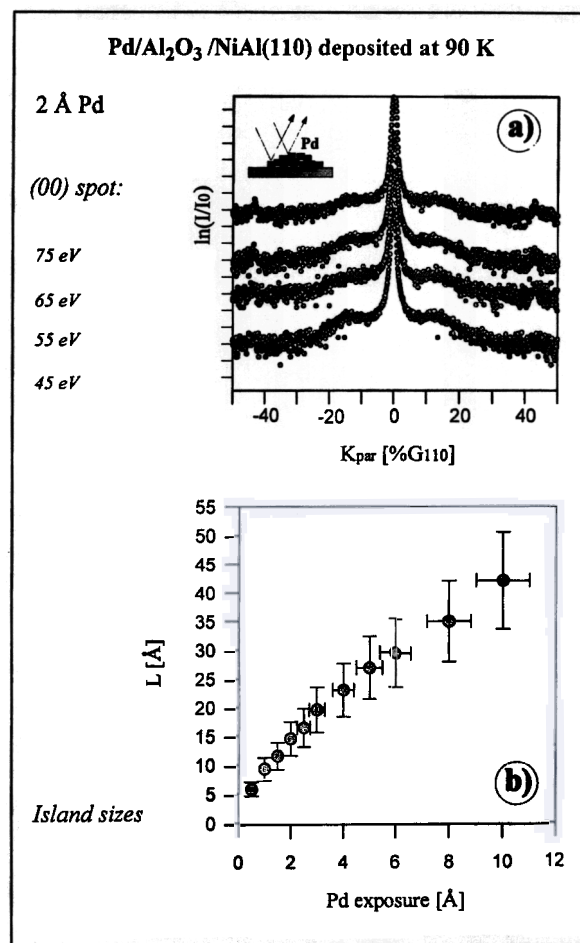


Fig. 4  
Deposition at 90 K: (a) LEED spot profiles of the (00) reflex for different energies. (b) Calculated island diameters (see appendix)

At 90 K, the growth mode appears to be totally different. Even at high coverages, no extra spots due to Pd were observed. Furthermore, the attenuation of the oxide LEED pattern is more pronounced although still not compatible with a layer by layer growth. In Fig. 4a, a energy series of profiles belonging to the (00) reflex is depicted. Comparing them to the profiles at 300 K, two major differences are

detectable: first, the diffuse part is ring shaped here and, second, no significant changes can be observed as the energy varies.

According to the discussion above, the missing energy dependence allows the conclusion that the particles formed at 90 K are probably disordered (see inset). In addition to that, the occurrence of a ring-shaped shoulder reveals a peaked island distance distribution.

Since disordered or amorphous areas on a surface usually have negligible scattering factors, the profiles can be described with the same two-layer model as used for the (111) crystallites at 300 K. Applying the same data analysis procedure, the particle sizes plotted in Fig. 4 b are obtained: obviously, the aggregates are much smaller than at 300 K. Moreover, it seems as if the growth law is different. (It should be taken into consideration, however, that the island sizes calculated for deposition at 90 K are less reliable as explained in the appendix.)

Again, the STM measurements confirm the LEED findings. Fig. 5 contains a representative image showing small aggregates attached to step edges or domain boundaries. Apparently, nucleation takes place at defects of the substrate even at 90 K.

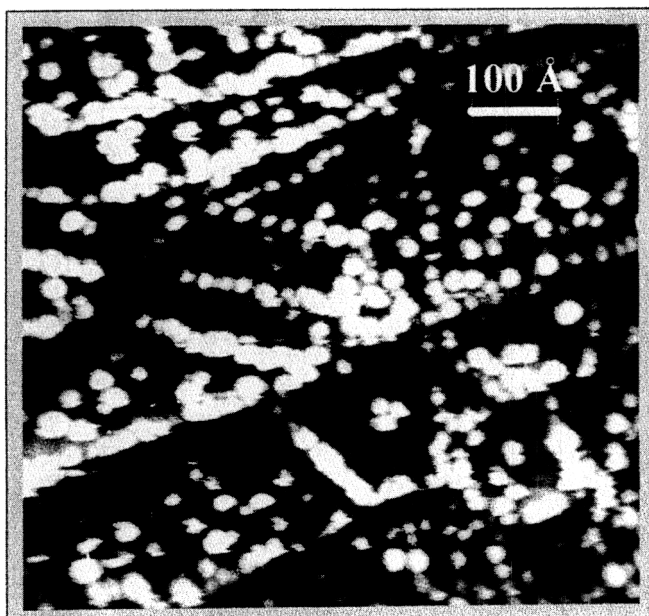


Fig. 5  
STM image (CCT,  $U = 1.6$  V,  $I = 2.2$  nA) of the Pd particles deposited at 90 K

### 3.2 Deposition of Pd: Adsorption of CO

The adsorption of CO was investigated via thermal desorption spectroscopy. The spectra have been obtained by exposing the sample to 20 L CO at 90 K and heating it to 800 K. Before discussing the results, it should be mentioned however that the metal deposits are not stable under the thermal treatment: as discussed in detail elsewhere [7], dif-

fusion of Pd into the oxide sets in at 400 K resulting in a nearly Pd-free surface at 800 K.

Fig. 6 surveys the situation for different Pd exposures at both deposition temperatures. The spectrum for the clean oxide has also been included for comparison: obviously, no CO desorption (and adsorption) takes place in the temperature range which is of interest here.

The most remarkable phenomena visible in the spectra of the Pd deposits are the following:

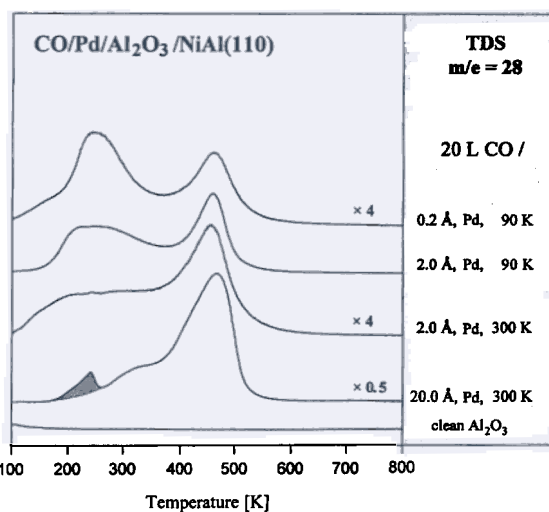


Fig. 6  
TD spectra for different amounts of Pd deposited at 300 K and 90 K and the clean alumina film after exposure of 20 L CO. The feature marked grey in the spectrum of the 20 Å deposit was identified as an artefact caused by coadsorption of hydrogen from the residual gas atmosphere

- The total amount of CO desorbing from the particles grown at 90 K is much higher as compared to the crystallites formed at 300 K for the same Pd exposure (note the scaling factors!).
- The features showing up at low temperatures (150–350 K) gain intensity as the particle size decreases at low metal exposures. This trend appears to be identical for both deposition temperatures.

The first observation can easily be explained by the different growth modes: since the aggregates are smaller at 90 K, they exhibit a larger total surface area for the adsorbing CO molecules. The second point will be discussed in Section 4.

### 3.3 Deposition of Pt

Since growth and adsorption properties of Pt on the alumina film have been described in detail elsewhere [5], a short summary is sufficient within the scope of this paper. It will demonstrate that the situation for Pt differs from the behaviour of Pd:

- At 300 K, the deposition of small amounts of Pt onto the film results in the formation of small two-dimensional

islands (10 – 20 Å) [8]. In contrast to Pd, a strong interaction between Pt and the oxide substrate is provable via LEED [8], HREELS and UPS [9].

- Experiments at a substrate temperature of 90 K revealed that the situation is similar to the deposition at room temperature as far as the growth mode is concerned: also in this case small two-dimensional islands are formed in the low coverage regime [8]. The substrate particle interaction, however, is less pronounced.
- Taking thermal desorption spectra of CO, it turns out that in the case of small Pt exposures deposited at 300 K a desorption feature at low temperature (~ 150 K) shows up in addition to a dominating peak at ~ 480 K. The low temperature feature is visible neither for deposition at 90 K nor for large amounts of Pt deposited at 300 K.

#### 4. Discussion

The results presented in Section 3 reveal interesting relationships between the structure of Pd and Pt deposits on Al<sub>2</sub>O<sub>3</sub>(111)/NiAl(110) and the adsorption of CO. Obviously, size effects and the particle-substrate interaction play a different role in both cases.

For Pd we find a three-dimensional growth mode at 300 K resulting in (111) crystallites on the surface. At 90 K, on the other hand, smaller, less ordered aggregates are formed. Nevertheless, similar trends can be observed in the TD spectra for both situations: apart from a peak at ~ 470 K, governing the spectrum for large particles, features between 150 K and 350 K gain intensity and become dominating with decreasing particle size.

In order to explain this size dependence, it is useful to consider the desorption behaviour of Pd single crystals first. TDS experiments for Pd(111) demonstrate that shoulders below the main desorption peak at ~ 500 K are also apparent in these spectra for high CO coverages [10]. The exact shape of the spectra depends on the adsorption temperature. IR and LEED measurements revealed that the low temperature desorption is due to the occurrence of repulsive interactions between the molecules leading to the occupation of new adsorption sites – identified as on-top sites – at high CO coverages ([10] and references therein).

Consequently, the changes in the TD spectra may be attributed to a higher degree of CO-CO interaction on the small particles, possibly also involving other adsorption geometries. (For small Pd particles on SiO<sub>2</sub>, for example, an increased population of terminal, on top sites was detected via IR spectroscopy [11].) We have carried out electron spectroscopic measurements supporting this interpretation [12]: they point towards a higher degree of coordination of the Pd atoms with CO molecules in case of very small aggregates grown at 90 K. Obviously, this may cause stronger repulsive CO-CO interactions and, in addition to that, induce a weakening of the Pd – CO bond.

Interestingly, TD spectra comparable to ours have also been obtained by other groups for small Pd particles – the particle diameters are comparable to those in this study –

deposited on  $\alpha$ -Al<sub>2</sub>O<sub>3</sub> single crystals (Al<sub>2</sub>O<sub>3</sub>(0001): [13], Al<sub>2</sub>O<sub>3</sub>( $\bar{1}$ 012): [14]) and on a  $\gamma$ -Al<sub>2</sub>O<sub>3</sub>-film [15]. Although the TD spectra shown in these publications were recorded with a starting temperature of 300 K, the authors also observe shoulders below 500 K which grow into the predominant peaks as the particle sizes decrease. Obviously, the adsorption behaviour of the Pd deposits are rather independent of the nature of the alumina substrate.

For Pt, the situation is different. Here, we observe the formation of small two-dimensional islands interacting strongly with the substrate for deposition at 300 K. These particles exhibit CO desorption spectra which show an instructive difference when related to TD spectra of Pt single crystals: apart from peaks in the range between 400 and 500 K, which are typical for CO/Pt, a desorption peak at rather low temperature, not apparent in the spectra of single crystals, emerges with decreasing island size.

This is the more surprising as small Pt particles on  $\alpha$ -Al<sub>2</sub>O<sub>3</sub> give rise to TDS peaks at higher temperatures imaging the behaviour of stepped Pt surfaces or Pt surfaces with defects [16].

Therefore, it is reasonable to attribute the feature to the particle substrate interaction probably causing significant changes in the electronic structure of the particles. This explanation is also corroborated by CO adsorption experiments on transition metal oxides which showed that desorption temperatures in the range between 150 K and 200 K are typical for these surfaces [17, 18].

Financial support of the following agencies is gratefully acknowledged: Deutsche Forschungsgemeinschaft, Ministerium für Wissenschaft und Forschung des Landes Nordrhein-Westfalen, Bundesministerium für Forschung und Technologie, Fonds der chemischen Industrie. Furthermore, J.L. thanks the Studienstiftung des deutschen Volkes for a fellowship and A.S. is grateful to the Swedish Natural Science Council (NFR) for financial support.

#### Appendix: Evaluation of the LEED Profiles

As all diffuse profiles observed in this study were found to be isotropic within the experimental accuracy, a one-dimensional scan was sufficient to reconstruct the two-dimensional intensity distribution of the diffuse shoulder. After a one-dimensional integration of this distribution, profiles were obtained, which correspond to the Fourier transforms of the one-dimensional pair correlation along straight lines on the surface.

As described in the literature, the diffuse shoulder for a one-dimensional problem can be easily calculated even for arbitrary size distributions [19]. (For this study gamma distributions for island sizes and island distances were assumed.) With the help of this formalism, it is possible to extract island sizes from LEED profiles by calculating profiles and comparing them to the experimental results. Using a fitting algorithm, the parameters can be varied until the best agreement between experiment and theory is achieved.

This procedure, however, requires additional information: namely, the fraction of the substrate covered by islands. In the present case, this piece of information was provided by the intensity of the oxide LEED pattern. As the metal islands do not significantly scatter into the directions of the oxide reflexes, the intensity of the central spike of the oxide spots is proportional to the square of the uncovered area [6]. Nevertheless, it is worth noting that this evaluation contains errors if the islands are small and thin so that they cannot safely be considered as "black holes".

Finally, it should be mentioned that the island sizes obtained from the fitting procedure are too small and have to be corrected: within the one-dimensional treatment all possible cuts through the islands – also those not going through the centre – are considered. Thus, the mean island length resulting from these cuts is smaller than the actual diameter of the two-dimensional islands.

## References

- [1] A.B. Stiles (ed.), *Catalyst Supports and Supported Catalysts*, Butterworths, Boston, 1987.
- [2] D.A. King and D.P. Woodruff (eds.), *The Chemical Physics of Solid Surfaces and Heterogenous Catalysis*, Vol. 3, Elsevier, Amsterdam, 1990.
- [3] J. Libuda, F. Winkelmann, M. Bäumer, H.-J. Freund, Th. Bertrams, H. Neddermeyer, and K. Müller, *Surf. Sci.* **318**, 61 (1994).
- [4] R.M. Jaeger, H. Kuhlenbeck, H.-J. Freund, M. Wuttig, W. Hoffmann, R. Franchy, and H. Ibach, *Surf. Sci.* **259**, 253 (1991).
- [5] F. Winkelmann, S. Wohlrab, J. Libuda, M. Bäumer, D. Cappus, M. Menges, K. Al-Shamery, H. Kuhlenbeck, and H.-J. Freund, *Surf. Sci.* **307–309**, 1148 (1994).
- [6] J. Wollschläger, J. Falta, and M. Henzler, *Appl. Phys. A* **50**, 57 (1990).
- [7] A. Sandell, J. Libuda, M. Bäumer, and H.-J. Freund, submitted to *Surf. Sci.*
- [8] J. Libuda, M. Bäumer, and H.-J. Freund, *J. Vac. Sci. Technol. A* **12**, 2259 (1994).
- [9] S. Wohlrab, F. Winkelmann, H. Kuhlenbeck, and H.-J. Freund, to appear in: *Springer Proceedings in Physics*, Springer, Berlin 1995.
- [10] X. Guo and J.T. Yates Jr., *J. Chem. Phys.* **90**, 6761 (1989).
- [11] X. Xu, D.W. Goodman, *Catal. Lett.* **24**, 31 (1994).
- [12] A. Sandell, J. Libuda, P. Brühwiler, S. Andersson, A. Maxwell, M. Bäumer, N. Märtensson, and H.-J. Freund, to appear in: *J. Electron Spectrosc. Relat. Phenom.*
- [13] H. Cordatos, T. Bunluesin, and R. J. Gorte, *Surf. Sci.* **323**, 219 (1995).
- [14] S. Ladas, H. Poppa, and M. Boudart, *Surf. Sci.* **102**, 151 (1981).
- [15] I. Stará and V. Matolín, *Surf. Sci.* **313**, 99 (1994).
- [16] E.I. Altman and R.J. Gorte, *Surf. Sci.* **195**, 392 (1988).
- [17] D. Cappus, J. Klinkmann, H. Kuhlenbeck, and H.-J. Freund, *Surf. Sci.* **325**, L421 (1995).
- [18] H. Kuhlenbeck, C. Xu, B. Dillmann, M. Haßel, B. Adam, D. Ehrlich, S. Wohlrab, H.-J. Freund, U.A. Ditzinger, H. Neddermeyer, M. Neuber, and M. Neumann, *Ber. Bunsenges. Phys. Chem.* **96**, 15 (1992).
- [19] P.R. Pukite, C.S. Lent, and P.I. Cohen, *Surf. Sci.* **161**, 39 (1985).

Presented at the 94th Annual Meeting of the Deutsche Bunsen-Gesellschaft für Physikalische Chemie "Reaktivität und Dynamik an Festkörperoberflächen" in Bremen, from May 25th to May 27th, 1995

E 9007